HHS Public Access

Author manuscript

J Immunol. Author manuscript; available in PMC 2019 June 01.

Published in final edited form as:

J Immunol. 2018 June 01; 200(11): 3711–3719. doi:10.4049/jimmunol.1700417.

PD-L1/B7-H1 inhibits viral clearance by macrophages in HSV-1-infected corneas

Sohyun Jeon[#,*,†], **Alexander M. Rowe**[#,*], **Kate L. Carroll**[*,‡], **Stephen A. K. Harvey**[*], and **Robert L. Hendricks**[*,§]

[*]University of Pittsburgh School of Medicine, Department of Ophthalmology, Pittsburgh, PA 15213

[†]Graduate program in Immunology, Pittsburgh, PA 15213

[‡]Graduate Program in Microbiology and Immunology, Pittsburgh, PA 15213

[§]Departments of Immunology and Microbiology and Molecular Genetics, Pittsburgh, PA 15213

Abstract

Immune privilege helps protect the cornea from damaging inflammation but can also impair pathogen clearance from this mucosal surface. Programmed death-ligand 1 (PD-L1 or B7-H1) contributes to corneal immune privilege by inhibiting the function of a variety of immune cells. We asked if PD-1/PD-L1 interaction regulates HSV type 1 (HSV-1) clearance from infected corneas. We show that PD-L1 is constitutively expressed in the corneal epithelium and is up-regulated upon HSV-1 corneal infection, with peak expression on $CD45^+$ cells NK cells, dendritic cells, neutrophils, and macrophages) and $CD45^-$ corneal epithelial cells at 4 days post infection (dpi). As early as 1 dpi, HSV-1 infected corneas of B7-$H1^{-/-}$ mice as compared to wild type mice showed increased chemokine expression and this correlated with increased migration of inflammatory cells into the viral lesions and decreased HSV-1 corneal titers. Local PD-L1 blockade caused a similar increase in viral clearance, suggesting a local effect of PD-1/PD-L1 in the cornea. The enhanced HSV-1 clearance at 2 dpi resulting from PD-1/PD-L1 blockade is mediated primarily by a monocyte/macrophage population. Studies in bone marrow chimeras demonstrated enhanced viral clearance when PD-L1 was absent only from non-hematopoetic cells. We conclude that PD-L1 expression on corneal cells negatively impacts the ability of the innate immune system to clear HSV-1 from infected corneas.

Introduction

The cornea is a clear, avascular tissue that covers the front of the eye. As a mucosal surface that is constantly exposed to the environment, the cornea is a potential portal of entry into the eye for pathogenic microorganisms. Indeed, the cornea utilizes physical barriers (tear film, epithelial tight junctions, etc.), chemical inhibitors such as defensins, and molecular and cellular innate and adaptive immune components to prevent invasion of ocular pathogens (1). However, inflammation is antithetical to corneal clarity, which is essential for

Corresponding Author: Robert L. Hendricks, University of Pittsburgh, Eye and Ear Institute Rm 919, 203 Lothrop Street, Pittsburgh PA 15213, USA' hendricksrr@upmc.edu.

[#]Both these authors contributed equally to this work

clear vision. Thus, the need for immune protection must be balanced by a corresponding need for immune privilege. Accordingly, the cornea has acquired multiple mechanisms to inhibit inflammation, including constitutive expression on corneal cells of PD-L1 (also called B7-H1), a ligand for the inhibitory programmed death-1 (PD-1) receptor (2–4). The degree, if any, to which the immune privilege of the cornea mediated through PD-L1 compromises immune protection requires clarification in experimental models of infectious disease.

HSV-1 corneal infections can result in epithelial lesions caused by virus replication in and destruction of corneal epithelial cells (5). These epithelial lesions represent the most common form of herpes keratitis in humans. Here we investigated the effect of blocking the PD-1/PD-L1 inhibitory interaction on the efficiency of HSV-1 clearance from the cornea. We found that both local administration of anti-PD-L1 blocking antibody and genetic deficiency in PD-L1 in B7-H1$^{-/-}$ mice significantly enhanced HSV-1 clearance from corneas of C57BL/6 mice. The enhanced HSV-1 clearance was associated with rapid leukocytic infiltration into the cornea, did not require PD-L1 expression on hematopoetic cells, and was mediated by a monocyte/macrophage population.

Materials and Methods

Mice

Female 6 – 8 wk old wild type (WT) C57BL/6 mice were purchased from The Jackson Laboratory (Bar Harbor, ME). B7-H1$^{-/-}$ mice on a C57BL/6 background were provided by Dr. Lieping Chen (Yale University School of Medicine, New Haven, CT). All experimental animal procedures were reviewed and approved by the University of Pittsburgh Institutional Animal Care and Use Committee, and the animals were handled in accordance with guidelines established by Institutional Animal Care and Use Committee.

Virus and corneal infections

WT HSV-1 strain KOS, or a KOS-based recombinant expressing eGFP from the promoter for a viral immediate early (α), gene infected cell protein 0 (ICP0-eGFP, generated by Dr. Paul R. Kinchington, University of Pittsburgh) were grown in Vero cells, and intact virions were isolated on Optiprep gradients according to the manufacturer's instructions (Accurate Chemical and Scientific, Westbury, NY). Mice were anesthetized by i.p. injection of 100 mg per kg of body weight ketamine hydrochloride and 0.1 mg per kg of body weight xylazine (Phoenix Scientific, San Marcos, CA) in 0.25 ml HBSS (BioWhittaker, Walkersville, MD). Mice received bilateral topical infection on scarified corneas with a dose of 1×10^5 PFU HSV-1 per cornea.

Antibodies and reagents for flow cytometry

PerCP-conjugated anti-CD45 (clone 30-F11) and PE-Cy7-conjugated anti–NK1.1 (clone PK136) were purchased from BD Pharmingen. PE-conjugated anti-PD-L1 (clone MIH5), allophycocyanin-conjugated anti–CD11c (clone N418), PE or allophycocyanin -eF780-conjugated anti–Gr-1 (clone RB6-8C5), PE-Cy7 or eFluor® 450-conjugated anti–F4/80 (clone BM8), and eFluor®450 or allophycocyanin conjugated CD11b (clone M1/70) were

purchased from eBioscience. Anti-PD-1 (clone RMP1-30) conjugated to PE-Cy7 was purchased from Biolegend (San Diego, CA). Appropriate isotype control antibodies were purchased from BD Pharmingen, eBioscience, or Biolegend. All flow cytometry data were collected on a FACSAria cytometer and analyzed by FlowJo software (FlowJo LLC, Ashland, Oregon). Macrophages and neutrophils were identified and distinguished using a multistep gating process. The $CD45^+$ cells were characterized into $CD11b^+$ and $CD11b^-$ populations that excluded $TCRbeta^+$ cells. The $CD11b^+$ cells were then divided based on Gr-1 expression into Gr-1 high ($Gr\text{-}1^{hi}$) and Gr-1 intermediate to low ($Gr\text{-}1^{int-low}$) groups. Macrophages were defined as $CD11b^+$ $Gr\text{-}1^{int-low}$ $F4/80^+$ $Ly6C^+$and neutrophils were defined as $CD11b^+Gr\text{-}1^{hi}$ $F4/80^{neg}$.

Corneal tissue preparation

Corneas were excised and processed under a dissecting microscope to separate the cornea and conjunctival tissue. The excised corneas were then digested in 100 μl per cornea of DMEM (Bio Whittaker) containing 0.2 U/ml of liberase TM (Roche) for 1 hour at 37°C, vortexing every 15 minutes followed by dispersal into single-cell suspensions by trituration through a p-200 pipette tip. The dispersed corneal cells were then stained and analyzed by flow cytometry. Alternatively, whole flat mounts of excised corneas were prepared and stained for confocal microscopic examination.

Generation of bone marrow chimeric mice

Bone marrow chimeras were created by tail vein transfer of 2×10^6 bone marrow cells from 6-wk-old WT or B7-$H1^{-/-}$ C57BL/6 mice into 6-wk-old lethally irradiated (2 × 500 rad treatments separated by 4 h rest) recipient mice. By this method, WT or B7-$H1^{-/-}$ mice were reconstituted with WT bone marrow (WT to WT) or (WT to B7-$H1^{-/-}$); and WT mice were reconstituted with B7-$H1^{-/-}$ bone marrow (B7-$H1^{-/-}$ to WT). The resulting chimeric mice were housed under immunocompromised mouse conditions for 8 wk after the transfer, and neomycin sulfate (2 mg/ml) from Sigma-Aldrich (St. Louis, MO) was added to their drinking water for 2 wk after the transfer. Bone marrow chimeras were fully reconstituted after 8 wk (6).

Quantification of infectious HSV-1

Mouse corneas were swabbed with sterile Weck-Cel surgical spears (Beaver Visitec, Waltham, MA) at various times after HSV-1 corneal infections, and spears were placed in 0.5 ml HBSS and frozen at −80°C until assayed. Dilutions of samples were added to confluent Vero cells, incubated for 1 h at 37°C, and overlaid with 0.5% methylcellulose. The cultures were incubated for 48 h, fixed with formalin, stained with crystal violet, and viral plaques were counted with the aid of a dissecting microscope.

In vivo treatments

Local antibody treatment restricted to the cornea was achieved through subconjunctival injections, while intraperitoneal (i.p.) injections were used for systemic treatment. Local PD-1/PD-L1 blockade or mock blockade was achieved by subconjunctival injections of 30 ng anti-PD-L1 (clone 10F.9G2, BioXCell) or control antibody, respectively. Local cellular

depletions were accomplished as previously described (7). Briefly, neutrophils were depleted or mock depleted with 50 μg anti-Ly6G (clone IA8) (BioXCell West Lebanon NH) or control antibody, monocytes/macrophages were depleted or mock depleted with 20 μL of clodronate liposomes and 70μg of purified anti-Ly6C (clone MONTS1) (BioXCell, West Lebanon NH) or 20 μl of PBS liposomes, and natural killer (NK) cell were depleted with 30 ng of anti-ASGM-1 antibody. Systemic PD-1/PD-L1 blockade or mock blockade was achieved through i.p. injection of 200 μg of anti-PD-L1 or control antibody. All treatments were performed at the time of HSV-1 infection.

Whole mount fluorescent confocal microscopy

Whole corneas were excised, washed in PBS + 4% FBS, fixed in 1% paraformaldehyde for 2 h, washed again in PBS + 4% FBS, incubated in Fc Block (BD, San Jose, CA) for 1 h, and then incubated with staining antibodies in PBS overnight at 4°C. The next day, corneas were extensively washed in PBS and then were flattened by making radial incisions and mounted. Images were acquired on an Olympus Fluoview 1000× confocal microscope with a 0.85 NA 20× oil objective. Images were acquired by sequential scanning to avoid fluorescence crossover, and Z stacks were acquired at Nyquist sampling frequency through the tissue. All image reconstructions were made using Olympus Fluoview.

Measurement of transcripts for inflammatory mediators in infected corneas

Total RNA was extracted from infected corneas using Qiagen's RNA extraction kit according manufacturer's protocol. Samples of total RNA (100 ng) were submitted to the University of Pittsburgh Genomics and Proteomics Core laboratory (GPCL) for analysis using the Nanostring system (Nanostring Technologies, 530 Fairview Avenue N, Seattle, WA 98109). Samples were hybridized overnight to a Codeset of synthetic capture probes and reporter probes capable of simultaneously detecting and quantifying mRNA encoding multiple inflammatory mediators.

RESULTS

PD-1/PD-L1 interaction inhibits HSV-1 clearance from infected corneas

Wild type (WT) or B7-H1$^{-/-}$ C57BL/6 mice received bilateral corneal infections with HSV-1 KOS, and viral titers were quantified in the tear film (Fig. 1A). Mean viral titers were significantly reduced in B7-H1$^{-/-}$ mice relative to WT mice at 1, 2, and 4 dpi. At 1 dpi, viral titers in WT mice were quite variable, but when compared to B7-H1$^{-/-}$ mice the difference in mean titers approached statistical significance ($p = 0.054$). HSV-1 titers increased and became less variable in WT mice by 2 dpi, with all corneas exhibiting HSV-1 titers greater than 5,000 pfu. Viral titers in B7-H1$^{-/-}$ mice remained relatively constant from 1-2 dpi, with only 6 of 17 corneas showing HSV-1 titers greater than 5,000 pfu and mean titers that were significantly ($p = 0.0001$) lower than those in WT mice. The HSV-1 titers decreased in both WT and B7-H1$^{-/-}$ mice from 2-4 dpi. By 4 dpi titers were very low in both groups, but were significantly ($p = 0.049$) lower in corneas of B7-H1$^{-/-}$ mice with 7 of 9 corneas showing complete viral clearance as compared with 2 of 6 WT corneas. Thus, HSV-1 clearance was significantly accelerated in B7-H1 compared to WT corneas from 1-4 dpi.

It was important to determine if the increased viral clearance in B7-H1$^{-/-}$ mice resulted specifically from the lack of PD-L1 expression in the cornea and to rule out the possibility that an unknown mutation in B7-H1$^{-/-}$ mice led to increased viral clearance. Therefore, PD-L1 was blocked locally in corneas of WT mice by subconjunctival injection of anti-PD-L1 antibody at the time of infection and HSV-1 titers were measured in the tear film at 1 and 3 dpi (Fig. 1B). Local in vivo PD-L1 blockade in the cornea decreased viral titers at both 1 dpi ($p = 0.053$) and 3 dpi ($p = 0.006$) compared to PBS-treated controls. As expected, B7-H1$^{-/-}$ mice also showed significantly reduced viral titers relative to PBS-treated WT mice at both 1 dpi ($p = 0.024$) and 3 dpi ($p = 0.018$). Viral titers were not significantly different in corneas in which B7-H1 was blocked locally in the cornea compared to titers in B7-H1$^{-/-}$ corneas. Thus, local PD-L1 expression specifically in the cornea is crucial for inhibiting viral clearance.

PD-L1 expression is upregulated in HSV-1 infected corneas

Corneas were excised from non-infected WT mice, or from HSV-1 infected WT mice at 1, 4, and 7 dpi. Flat mounts were stained for PD-L1 and examined with a confocal microscope. Representative images (Fig. 2A) reveal low levels of PD-L1 expression in non-infected corneal epithelium as previously reported [2]. PD-L1 expression was transiently up-regulated in the corneal epithelium following HSV-1 corneal infection, with peak expression levels observed at 4 dpi (Fig 2A).

To examine the PD-L1 expression on subsets of infiltrating immune cells, corneas were excised from HSV-1 infected WT mice at 2 and 4 dpi and spleens were excised at 4 dpi. The dispersed cells were stained, gated on CD45^{+} cells, and PD-L1 expression was assessed on NK1.1^{+} NK cells, CD11c^{+} dendritic cells (DC), Gr-1^{high}, F4/80^{-} neutrophils, and Gr-1$^{int\text{-}low}$ F4/80^{+} macrophages by flow cytometry (Fig. 2B). In the cornea, PD-L1 was highly expressed on all leukocyte populations tested. The mean frequency of PD-L1^{+} cells increased in all leukocyte populations in the cornea from 2-4 dpi, but the increase achieved statistical significance only within the NK and DC populations. At 4 dpi, the frequency of PD-L1 expression in all leukocyte populations was significantly higher in the cornea than on their counterparts in the spleen, suggesting that PD-L1 expression is upregulated when leukocytes infiltrate infected corneas.

Disruption of PD-1/PD-L1 interaction increases chemokine expression and leukocytic infiltration in infected corneas

We hypothesized that the enhanced clearance of HSV-1 seen in corneas of B7-H1$^{-/-}$ mice was due to increased corneal inflammation in the absence of PD-1/PD-L1 interaction. Total corneal RNA was extracted at 1 dpi and transcripts quantified by nanostring®. Transcripts for chemokines and chemokine receptors that attract NK cells, inflammatory monocytes, and neutrophils such as CCL3, CXCL1, and CXCR3 as well as molecules that contribute to leukocytic extravasation from the blood (ICAM1, PECAM1) were up-regulated in the absence of PD-L1 (Fig. 3A). The increased chemokine gene expression was associated with a dramatic increase in leukocytic infiltration into the central corneas lacking PD-L1 expression. By using a recombinant HSV-1 KOS that expresses eGFP from a viral ICP0 promoter to infect corneas of B7-H1$^{-/-}$ and WT mice, we also show that the increased

chemokine and adhesion molecule gene expression in B7-H1$^{-/-}$ mice correlates with migration of CD45^{+} cells (most co-expressing Gr-1) into the central cornea in association with reduced expression of the viral promoter (Fig. 3B).

PD-1 expression on myeloid and non-myeloid cells in HSV-1 infected corneas

Both myeloid cells (macrophages, neutrophils) and non-myeloid cells NK cells rapidly infiltrate the cornea after HSV-1 infection (Fig. 4A), and we asked which of these populations expressed PD-1 and would thus be susceptible to PD-L1 regulation. HSV-1 infected corneas of WT and B7-H1$^{-/-}$ mice were excised at 2 and 4 dpi and single cell suspensions gated on CD45^{+} cells were analyzed for PD-1 expression on neutrophils, macrophages, and NK cells. The majority of neutrophils (CD11b^{+} Gr-1^{high} F4/80^{-}) in infected corneas of wild type and B7-H1$^{-/-}$ mice were PD-1 negative (Fig. 4B). Approximately 20-30% of macrophages (CD11b^{+} Gr-1$^{int-low}$ F4/80^{+}) expressed PD-1 in infected corneas (Fig. 4B&C). Although the percentage of macrophages expressing PD-1 tended to be higher at 4 dpi compared to 2 dpi, and in corneas of B7-H1$^{-/-}$ compared to WT mice, group and time differences in PD-1 expression on macrophages were not statistically significant. Approximately 20-45% of non-myeloid (CD11b^{-} Gr-1^{-} F4/80^{-}) cells expressed PD-1 and the frequency of PD-1 positive cells in non-myeloid cells was significantly higher in infected corneas of B7-H1$^{-/-}$ mice compared to WT mice (Fig. 4B&D).

Neutrophils do not mediate enhanced viral clearance from corneas of B7-H1$^{-/-}$ mice

Since neutrophils do not express PD-1 in infected corneas, we anticipated that depleting them by treating mice subconjunctivally with anti-Ly6G (clone IA8) at the time of infection would not abrogate the enhanced HSV-1 clearance from the corneas of B7-H1$^{-/-}$ mice observed at 2 and 4 dpi. The treatment effectively depleted CD45^{+} CD11b^{+} Gr-1^{high} cells (neutrophils) (Fig. 5A), but did not significantly deplete (CD11b^{high} Gr-1$^{low-int}$ macrophages/monocytes (Fig B&C). Neutrophil depletion had no impact on viral clearance in B7-H1$^{-/-}$ mice (Fig. 5D) or WT mice (data not shown).

PD-1/PD-L1 interactions do not regulate NK cell mediated clearance of HSV-1 from the cornea

We and others have established an important role for NK cells in the later stages (4 dpi) of HSV-1 clearance from infected corneas (8, 9). We proposed that NK cells might account for the enhanced HSV-1 clearance observed when PD-1/PD-L1 interaction was blocked in infected corneas. This hypothesis was based on the observations that 20-45% of non-myeloid cells express PD-1 at 2 and 4 dpi in infected corneas (Fig 4D), and that the frequency of non-myeloid cells expressing PD-1 was higher in B7-H1$^{-/-}$ mice (Fig 4D). Accordingly, B7-H1$^{-/-}$ mice received subconjunctival injections of anti-ASGM-1 antibody or a combination of anti-ASGM-1 and anti-PD-L1 antibodies to deplete NK cells alone or in combination with PD-1/PD-L1 blockade at the time of HSV-1 infection. At 4 dpi, corneas were swabbed for viral titers and then excised, dispersed into single cells, and analyzed by flow cytometry for the efficacy of NK cell and PD-L1^{+} cell depletion from infiltrating CD45 cells (Fig. 6). The anti-ASGM-1 and anti-PD-L1 treatment effectively depleted infiltrating NK cells, and depleted or blocked PD-L1 expression on infiltrating cells, respectively (Fig. 6A). While local NK cell-depletion alone significantly reduced HSV-1 clearance from the

cornea at 4 dpi, the combination of NK cell depletion and PD-L1 blockade completely compensated for this effect (Fig 6B). Thus, NK cells are not responsible for the enhanced HSV-1 clearance observed in the absence of PD-1/PD-L1 interaction, and in fact blocking PD-1/PD-L1 interaction can compensate for the reduced HSV-1 clearance in the absence of NK cells.

Monocytes/macrophages are responsible for enhanced HSV-1 clearance from corneas of B7-H1$^{-/-}$ mice

We next asked if local depletion of macrophages using combined subconjunctival injections of clodronate-liposomes and anti-Ly6C (clone MONTS1) on the day of infection would alter the enhanced HSV-1 clearance from corneas of B7-H1$^{-/-}$ mice. The treatment significantly reducedLy6C^{+} Gr-1$^{int-low}$ monocytes/macrophages from the cornea at 2 dpi (Fig. 7A). As expected, HSV-1 clearance was significantly enhanced ($p< 0.001$) in corneas of mock-depleted B7-H1$^{-/-}$ mice compared to mock-depleted WT mice at 2 dpi (Fig. 7B). Viral titers were significantly ($p < 0.001$) increased in B7-H1$^{-/-}$ mouse corneas that were depleted of macrophages (Fig. 7C). Macrophage depletion also increased viral titers in corneas of WT mice ($p = 0.055$). Macrophage depletion caused a significantly larger increase in viral titers in B7-H1$^{-/-}$ mice compared to WT mice, and titers in macrophage depleted B7-H1 and WT mice were not significantly different. These findings demonstrate that monocytes/macrophages are not only involved in HSV-1 clearance, but are responsible for the enhanced antiviral activity in corneas of B7-H1$^{-/-}$ mice at 2 dpi. We propose that the increased infiltration of monocytes/macrophages in mock depleted corneas of WT mice compared to B7-H1$^{-/-}$ mice at 2 dpi might reflect compensation for PD-1/PD-L1-induced functional compromise of monocyte/macrophages and the accompanying increase in viral titers.

As shown in Figure 1, viral clearance from corneas is nearly complete by 4 dpi, and the enhancing effect of PD-1/PD-L1 interaction, though statistically significant, is less pronounced. In these experiments the viral titers were very low in all groups at 4 dpi, and the inhibitory effect of PD-1/PD-L1 interaction was not apparent in these experiments (data not shown).

Enhanced HSV-1 clearance requires PD-L1 expression on non-hematopoietic cells

Since PD-L1 is expressed on both hematopoietic (Fig. 2B) and non-hematopoietic (Fig. 2A) cells in HSV-1 infected corneas, we sought to determine which type(s) of PD-L1 positive cell contributes to the enhanced viral clearance at 2 and 4 dpi. Accordingly, we created bone marrow chimeric mice by transferring either WT bone marrow cells into irradiated WT or B7-H1$^{-/-}$ mice or B7-H1$^{-/-}$ bone marrow into irradiated WT mice. The B7-H1$^{-/-}$ to WT chimeras showed similar HSV-1 clearance at 2 and 4 dpi to WT to WT chimeras (data not shown). However, chimeras comprised of WT bone marrow in B7-H1$^{-/-}$ mice exhibited enhanced viral clearance at both 2 and 4 dpi (Fig. 8). Thus, enhanced viral clearance from infected corneas requires PD-L1 expression only on non-hematopoietic cells.

Discussion

Following primary HSV-1 corneal infection the virus replicates in corneal epithelial cells forming characteristic dendritic or geographic shaped lesions. The duration of virus replication appears to vary somewhat with the strain of virus and the strain of mice used. In our hands, HSV-1 KOS or RE strains are largely cleared from the corneas of C57BL/6 mice by 4-6 dpi. In contrast, clearance of the HSV-1 McKrae strain from the corneas of C57BL/6 mice has been shown to take more than 7 days (10). The more rapid clearance of HSV-1 KOS and RE would suggest primary involvement of an innate immune response, while the slower clearance of the McKrae strain might suggest greater involvement of adaptive immunity. Thus, regulation of viral clearance might be different in corneas infected with different strains of virus.

The cornea exhibits a degree of immune privilege due to the constitutive expression of a variety of inhibitory molecules including PD-L1 (1–4). PD-L1 functions primarily by binding to PD-1 on effector cells (T cells, B cells, NK cells, macrophages etc) and delivering an inhibitory signal leading to functional impairment (11, 12). There is ample evidence that cells of the innate immune system such as macrophages, DCs, and NK cells express PD-1, and that their function can be negatively regulated by PD-1 signaling following binding of ligands such as PD-L1 (13–17). However, PD-L1 can also bind CD80 (18), and PD-L1 on naïve T cells is required for DC maturation, including CD80 expression on DCs (19). Decreased CD80 expression on lymph node dendritic cells through PD-L1 blockade has been associated with decreased expansion of HSV-specific $CD8^+$ T cells and delayed clearance of HSV-1 McKrae from corneas of C57BL/6 mice as measured at 7 dpi (10). PD-1/PD-L1 regulation of early viral clearance by the innate immune system was not examined in that study. Here we examined the effect of PD-L1 expression on the more rapid clearance of HSV-1 KOS from infected corneas.

We confirm previous findings (2) that PD-L1 is constitutively expressed on corneal epithelium and demonstrate that expression is increased following HSV-1 corneal infection, with peak expression at 4 dpi. We further demonstrate that innate immune cells including NK cells, DCs, neutrophils, and macrophages are recruited to the corneas of C57BL/6 mice within 2 days of HSV-1 KOS corneal infection. We observed that a much higher frequency of these innate immune cells express PD-L1 in the cornea when compared to their counterparts in the spleen, suggesting a general up-regulation of PD-L1 on both hematopoietic and non-hematopoietic cells in infected corneas. The expression of PD-L1 is regulated by type I and type II interferon, both of which are rapidly expressed in infected corneas (20–22).

Corneal whole mounts of B7-$H1^{-/-}$ mice infected with HSV-1 KOS that expresses eGFP from a viral immediate early promoter showed increased leukocytic migration towards the central cornea compared to WT mice, which correlated with significantly increased expression of chemokines and adhesion molecules associated with leukocytic extravasation. Moreover, the viral lesions appeared to be completely absent from the peripheral corneas and reduced in the central corneas of B7-$H1^{-/-}$ mice as early as 1 dpi, consistent with viral clearance by the advancing leukocytic infiltrate.

In our experiments HSV-1 KOS and RE strains are nearly cleared from mouse corneas by 4 dpi. We, and others have shown that NK cells contribute to HSV-1 clearance from corneas at late (4 dpi), but not earlier times after infection (9, 20). Our current study confirmed previous results showing that NK cell depletion significantly increases HSV-1 corneal titers at 4 dpi, but demonstrated that the increase was reversed by simultaneous PD-L1 blockade. Thus, PD-L1 blockade can augment HSV-1 clearance from the cornea at 4 dpi by an NK cell-independent mechanism. However, in some experiments HSV-1 clearance was nearly complete by 4 dpi even in corneas where PD-1/PD-L1 was not blocked, so that an enhancing effect of PD-1/PD-L1 interaction could not be observed. We conclude that PD-1/PD-L1 interaction primarily regulates very early clearance of HSV-1 from corneas at 2 dpi.

Ly6G is expressed at high levels on neutrophils and low levels on monocytes/macrophages. Local (subconjunctival) injection of anti-Ly6G antibody effectively reduced the number of neutrophils in infected corneas of B7-H1$^{-/-}$ mice, but did not significantly influence the monocyte/macrophage numbers. However, depleting neutrophils had no effect on HSV-1 clearance from corneas of B7-H1$^{-/-}$ or WT mice. This is consistent with the apparent lack of involvement of neutrophils in HSV-1 clearance from corneas of WT mice reported previously (20, 23), and their lack of involvement in HSV-1 clearance following nasal and skin infection observed by others (24, 25).

The F4/80^{+} Ly6C^{+}population is comprised of macrophages (Gr-1^{low}) and inflammatory monocytes (Gr-1^{int}), and both of these populations are present in the cornea early after HSV-1 infection (20, 26, 27). Systemic depletion of macrophages from mice with clodronate-liposomes was previously shown to significantly increase acute HSV-1 replication in the peripheral nervous system following HSV-1 corneal infection (28). We employed a previously established subconjunctival treatment of mice with a combination of clodronate-liposomes and anti-Ly6C antibody. This treatment has been shown to effectively eliminate tissue resident macrophages from corneas during latent HSV-1 infections (7). Although the monocyte/macrophage population was small in the infected cornea at 2 dpi, their depletion completely abrogated the enhanced HSV-1 clearance from the cornea, suggesting an important role for these cells in HSV-1 clearance from the cornea, and their requisite role in the enhanced clearance resulting from disruption of PD-1/PD-L1 interaction in the cornea.

Since PD-L1 is expressed on both resident corneal cells and on leukocytes that infiltrate the infected cornea within 2 days of HSV-1 infection, it was of interest to determine which cell type inhibited viral clearance through PD-L1. We employed bone marrow chimeric mice in which PD-L1 was knocked out on only bone marrow-derived cells or on only non-bone marrow-derived cells. The results showed an important role for PD-L1 expression on non-hematopoietic cells but not on hematopoietic cells for enhanced HSV-1 clearance from the cornea. Since PD-L1 is upregulated on corneal epithelial cells while they are supporting HSV-1 replication, it is likely that PD-L1 expression inhibits viral clearance from these cells by inflammatory monocytes or macrophages.

We conclude that PD-1/PD-L1 blockade enhances early HSV-1 clearance from the cornea by augmenting innate immunity. The improved clearance is seen as early as 1 day after

infection and is associated with increased expression of chemokines and adhesion molecules, and a more rapid and robust leukocytic infiltration of the central cornea. Although several cellular components of the innate immune system including NK cells, monocytes/macrophages, neutrophils, and DCs rapidly infiltrate the cornea after infection, it appears that PD-1/PD-L1 blockade augments viral clearance primarily by enhancing the antiviral activity of monocytes/macrophages. It should be noted that our studies involved a primary infection model. It remains to be determined if a similar effect would be observed with lesions resulting from reactivation of latent HSV-1, more commonly seen in humans. Nonetheless, our findings are consistent with the notion that short-term use of PD-L1 blocking reagents might have therapeutic efficacy for treating HSV-1 corneal epithelial disease.

Acknowledgments

The authors gratefully acknowledge the expert assistance of Moira Geary, Kira Lathrop, and Nancy Zurowski

Funding: Supported by National Eye Institute grants EY05945 (RLH), EY 026891 (RLH), P30 EY08098 (RLH), an unrestricted grant from Research to Prevent Blindness (New York, NY) and the Eye and Ear Foundation of Pittsburgh

Abbreviations in this article

PD-1	programmed death 1
PD-L1	PD-1 ligand
pfu	plaque forming units
ASGM-1	asialoGM-1
KOS	Kendal O Smith
WT	wild type

References

1. Knop E, Knop N. Anatomy and immunology of the ocular surface. Chem Immunol Allergy. 2007; 92:36–49. [PubMed: 17264481]
2. Hori J, Wang MC, Miyashita M, Tanemoto K, Takahashi H, Takemori T, Okumura K, Yagita H, Azuma M. B7-H1-induced apoptosis as a mechanism of immune privilege of corneal allografts. J Immunol. 2006; 177:5928–5935. [PubMed: 17056517]
3. Jun H, Seo SK, Jeong HY, Seo HM, Zhu G, Chen L, Choi IH. B7-H1 (CD274) inhibits the development of herpetic stromal keratitis (HSK). FEBS Lett. 2005; 579:6259–6264. [PubMed: 16253242]
4. Watson MP, George AJ, Larkin DF. Differential effects of costimulatory pathway modulation on corneal allograft survival. Invest Ophthalmol Vis Sci. 2006; 47:3417–3422. [PubMed: 16877411]
5. Rowe AM, St Leger AJ, Jeon S, Dhaliwal DK, Knickelbein JE, Hendricks RL. Herpes keratitis. Progress in retinal and eye research. 2013; 32:88–101. [PubMed: 22944008]
6. Jeon S, St Leger AJ, Cherpes TL, Sheridan BS, Hendricks RL. PD-L1/B7-H1 regulates the survival but not the function of CD8+ T cells in herpes simplex virus type 1 latently infected trigeminal ganglia. J Immunol. 2013; 190:6277–6286. [PubMed: 23656736]

7. Rowe AM, Yun H, Treat BR, Kinchington PR, Hendricks RL. Subclinical Herpes Simplex Virus Type 1 Infections Provide Site-Specific Resistance to an Unrelated Pathogen. J Immunol. 2017; 198:1706–1717. [PubMed: 28062697]
8. Frank GM, Buela KA, Maker DM, Harvey SA, Hendricks RL. Early responding dendritic cells direct the local NK response to control herpes simplex virus 1 infection within the cornea. J Immunol. 2012; 188:1350–1359. [PubMed: 22210909]
9. Inoue T, Inoue Y, Kosaki R, Inoue Y, Nishida K, Shimomura Y, Tano Y, Hayashi K. Immunohistological study of infiltrated cells and cytokines in murine herpetic keratitis. Acta Ophthalmol Scand. 2001; 79:484–487. [PubMed: 11594984]
10. Bryant-Hudson KM, Carr DJ. PD-L1-expressing dendritic cells contribute to viral resistance during acute HSV-1 infection. Clin Dev Immunol. 2012; 2012:924619. [PubMed: 22474484]
11. Bardhan K, Anagnostou T, Boussiotis VA. The PD1:PD-L1/2 Pathway from Discovery to Clinical Implementation. Front Immunol. 2016; 7:550. [PubMed: 28018338]
12. Haro MA, Littrell CA, Yin Z, Huang X, Haas KM. PD-1 Suppresses Development of Humoral Responses That Protect against Tn-Bearing Tumors. Cancer Immunol Res. 2016; 4:1027–1037. [PubMed: 27856425]
13. Qorraj M, Bruns H, Bottcher M, Weigand L, Saul D, Mackensen A, Jitschin R, Mougiakakos D. The PD-1/PD-L1 axis contributes to immune metabolic dysfunctions of monocytes in chronic lymphocytic leukemia. Leukemia. 2017; 31:470–478. [PubMed: 27479178]
14. Wang F, Huang X, Chung CS, Chen Y, Hutchins NA, Ayala A. Contribution of programmed cell death receptor (PD)-1 to Kupffer cell dysfunction in murine polymicrobial sepsis. Am J Physiol Gastrointest Liver Physiol. 2016; 311:G237–245. [PubMed: 27288425]
15. Della Chiesa M, Pesce S, Muccio L, Carlomagno S, Sivori S, Moretta A, Marcenaro E. Features of Memory-Like and PD-1(+) Human NK Cell Subsets. Front Immunol. 2016; 7:351. [PubMed: 27683578]
16. Huang BY, Zhan YP, Zong WJ, Yu CJ, Li JF, Qu YM, Han S. The PD-1/B7-H1 pathway modulates the natural killer cells versus mouse glioma stem cells. PLoS One. 2015; 10:e0134715. [PubMed: 26266810]
17. Yao S, Chen L. PD-1 as an immune modulatory receptor. Cancer J. 2014; 20:262–264. [PubMed: 25098286]
18. Butte MJ, Keir ME, Phamduy TB, Sharpe AH, Freeman GJ. Programmed death-1 ligand 1 interacts specifically with the B7-1 costimulatory molecule to inhibit T cell responses. Immunity. 2007; 27:111–122. [PubMed: 17629517]
19. Talay O, Shen CH, Chen L, Chen J. B7-H1 (PD-L1) on T cells is required for T-cell-mediated conditioning of dendritic cell maturation. Proc Natl Acad Sci U S A. 2009; 106:2741–2746. [PubMed: 19202065]
20. Frank GM, Lepisto AJ, Freeman ML, Sheridan BS, Cherpes TL, Hendricks RL. Early CD4(+) T cell help prevents partial CD8(+) T cell exhaustion and promotes maintenance of Herpes Simplex Virus 1 latency. J Immunol. 2010; 184:277–286. [PubMed: 19949087]
21. Hendricks RL, Weber PC, Taylor JL, Koumbis A, Tumpey TM, Glorioso JC. Endogenously produced interferon alpha protects mice from herpes simplex virus type 1 corneal disease. The Journal of general virology. 1991; 72(Pt 7):1601–1610. [PubMed: 1649898]
22. Conrady CD, Jones H, Zheng M, Carr DJ. A Functional Type I Interferon Pathway Drives Resistance to Cornea Herpes Simplex Virus Type 1 Infection by Recruitment of Leukocytes. J Biomed Res. 2011; 25:111–119. [PubMed: 21709805]
23. Royer DJ, Zheng M, Conrady CD, Carr DJ. Granulocytes in Ocular HSV-1 Infection: Opposing Roles of Mast Cells and Neutrophils. Invest Ophthalmol Vis Sci. 2015; 56:3763–3775. [PubMed: 26066745]
24. Wojtasiak M, Pickett DL, Tate MD, Bedoui S, Job ER, Whitney PG, Brooks AG, Reading PC. Gr-1+ cells, but not neutrophils, limit virus replication and lesion development following flank infection of mice with herpes simplex virus type-1. Virology. 2010; 407:143–151. [PubMed: 20817252]
25. Wojtasiak M, Pickett DL, Tate MD, Londrigan SL, Bedoui S, Brooks AG, Reading PC. Depletion of Gr-1+, but not Ly6G+, immune cells exacerbates virus replication and disease in an intranasal

model of herpes simplex virus type 1 infection. The Journal of general virology. 2010; 91:2158–2166. [PubMed: 20538903]

26. Austyn JM, Gordon S. F4/80, a monoclonal antibody directed specifically against the mouse macrophage. Eur J Immunol. 1981; 11:805–815. [PubMed: 7308288]
27. Lagasse E I, Weissman L. Flow cytometric identification of murine neutrophils and monocytes. J Immunol Methods. 1996; 197:139–150. [PubMed: 8890901]
28. Kodukula P, Liu T, Rooijen NV, Jager MJ, Hendricks RL. Macrophage control of herpes simplex virus type 1 replication in the peripheral nervous system. J Immunol. 1999; 162:2895–2905. [PubMed: 10072539]

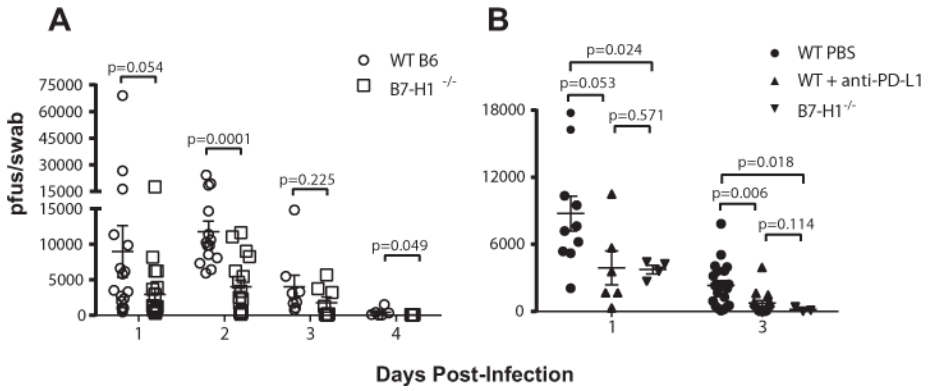

Figure 1. PD-1/PD-L1 interactions regulate HSV-1 clearance from infected corneas

(**A**) WT or B7-H1$^{-/-}$ C57BL/6 mice were bilaterally infected with HSV-1 KOS. At various days post-infection the corneas were swabbed, infectious HSV-1 was quantified in a viral plaque assay, and data are recorded as plaque forming units (pfu)/swab ± SEM. For WT mice n = 20 mice at 1 dpi, n=14 mice at 2 dpi, n= 8 mice at 3 dpi and n= 6 mice at 4 dpi; for B7-H1−/− mice n = 20 mice at 1 dpi, n = 17 mice at 2 dpi, n = 8 mice at 3 dpi and n = 9 mice at 4 dpi. (**B**) Corneas of WT or B7-H1$^{-/-}$ C57BL/6 mice were infected with HSV-1. At the time of infection WT mice received a subconjunctival injection of anti-PD-L1 or PBS. Corneas were swabbed at 1 and 3 dpi, infectious HSV-1 was quantified in a viral plaque assay, and data are recorded as pfu/swab ± SEM. Mann-Whitney tests were used to assess the significance of differences at individual days.

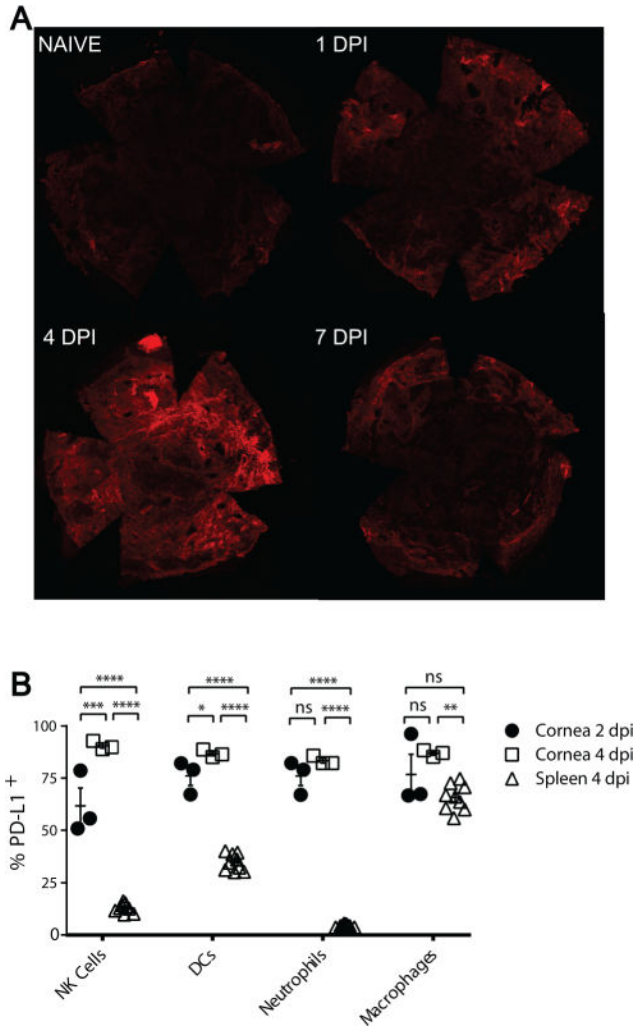

Figure 2. PD-L1 is rapidly upregulated in the cornea after HSV-1 infection

Corneas of WT C57BL/6 mice were infected with HSV-1 and (**A)** were excised at various days post-infection (dpi), stained for PD-L1, and flat mounts were analyzed by confocal microscopy. A representative photomicrograph shows the level of PD-L1 expression on corneal epithelium increased following infection, peaking at 4 dpi. **(B)** Single cell suspensions of pooled corneas obtained at 2 and 4 dpi or spleen cells obtained at 4 dpi were stained for CD45 (all leukocytes), NK1.1 (NK cells), CD11c (Dendritic Cells), Gr-1^{High}, F4/80^{-} (Neutrophils), F4/80^{+},Gr-$1^{int\text{-}low}$ (Macrophages) and PD-L1 and were analyzed by flow cytometry. The cells were gated on CD45 and the frequency of PD-L1 positive cells within each leukocyte subpopulation was assessed in 3 pools of 6 corneas and 9 spleens. The significance of group differences was assessed using a one-way ANOVA with Tukey's post-tests (*$p< 0.05$, **$p < 0.01$, ***$p < 0.001$, ****$p<0.0001$, ns $p> 0.05$)

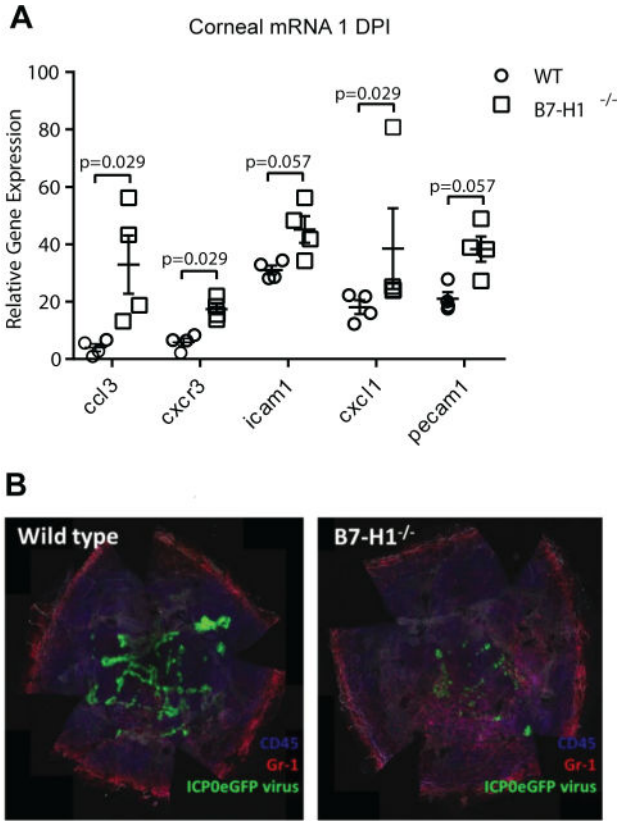

Figure 3. PD-L1 regulates expression of chemokines, adhesion molecules, and viral genes expression in infected corneas

(**A**) Corneas of WT and B7-H1$^{-/-}$ mice were infected with HSV-1 KOS, excised 1 day after infection, total mRNA was extracted, and the levels of specific mRNAs were assessed by Nanostring^{R} (n=4 mice per group). Mouse genotype significantly influenced overall gene expression ($p<0.0001$, two-way ANOVA). Shown are those genes whose expression differed substantially between WT and B7-H1$^{-/-}$ mice as assessed by a Mann Whitney Rank Sum Test. (**B**) Corneas of WT and B7-H1$^{-/-}$ mice were infected with a recombinant HSV-1 KOS that expresses eGFP under the immediate early ICP0 viral promotor. The corneas were excised 1 day after infection, stained for CD45 (blue) and Gr-1 (red) and analyzed by confocal microscopy. A representative photomicrograph shows dramatically reduced viral gene expression in corneal epithelial cells (green) and increased infiltration of mainly CD45^{+}, Gr-1^{+} cells into the central cornea of B7-H1$^{-/-}$ mice.

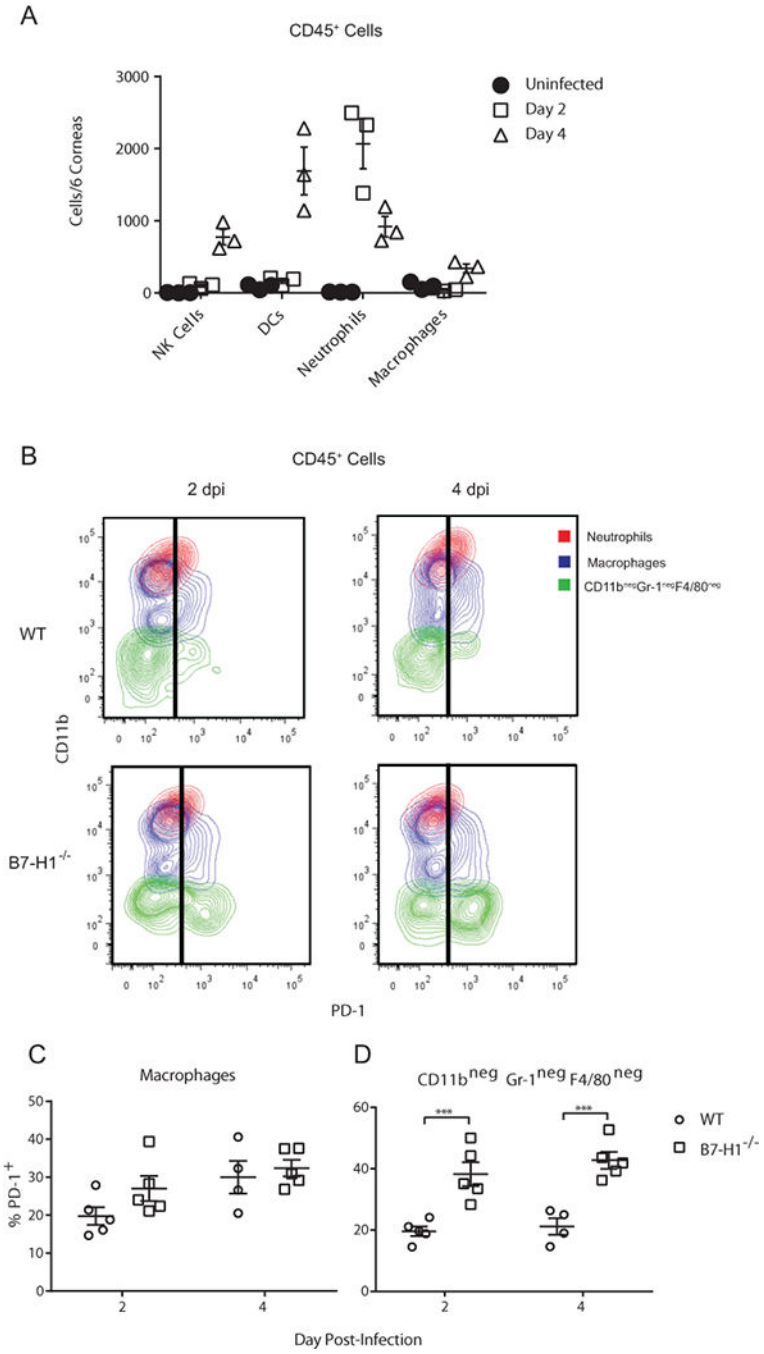

Figure 4. Expression of PD-1 by infiltrating immune cells

(A) Corneas of wild type mice were not infected or infected with HSV-1 KOS. At 2 and 4 dpi corneas were excised, single cell suspensions of pools of 6 corneas were stained for CD45 (leukocytes), NK1.1 (NK cells), CD11c (DC), Gr-1 (neutrophils, inflammatory monocytes), F4/80 (macrophages), and for PD-1. A defined number of fluorescent beads were added to each cell sample to determine absolute cell numbers. Samples were gated on CD45 and the number of each leukocyte subpopulation in each pool of 6 corneas was determined by flow cytometry. **(B-D)** Corneas of wild type and B7-H1$^{-/-}$ mice were infected

with HSV-1 KOS. At 2 and 4 dpi corneas were excised, single cell suspensions were prepared, stained for CD11b, Gr-1, F4/80, and PD-1 and analyzed by flow cytometry**(B)** Representative flow plots gated on CD45 cells illustrate levels of PD-1 expression on neutrophils (large, granular $CD11b^{high}$ $Gr\text{-}1^{high}$ $F4/80^{-}$), macrophages ($CD11b^{+}$, $F4/80^{int-low}$), and non-myeloid cells ($CD11b^{-}$ $Gr\text{-}1^{-}$, F4/80). Little or no PD-1 expression was detected on neutrophils. Scatter plot shows the frequency of $PD\text{-}1^{+}$ cells within the **(C)** macrophage gate and **(D)** non-myeloid cell gate. The significance of differences between genotypes at individual days in C & D was assessed by a two-way ANOVA with Sidak's post-tests (***$p<0.001$).

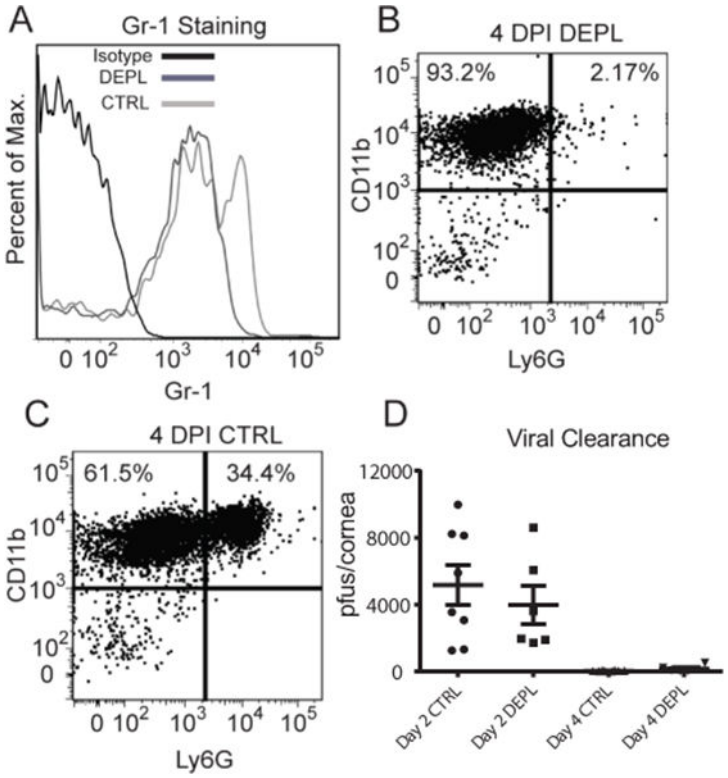

Figure 5. Effect of neutrophil depletion on HSV-1 clearance from corneas of B7-H1 KO mice

B7-H1$^{-/-}$ mice received subconjunctival injections of a control antibody or anti-Ly6G antibody (clone IA8) to locally deplete neutrophils at the time of HSV-1 corneal infection. **(A)** Corneas that received subconjectivial injections of IA8 were excised at 2 DPI and single cell suspensions were stained for CD45, CD11b, and Gr-1 (clone RB6) and analyzed by flow cytometry. The IA8 treatment (DEPL-dark grey line) removed the Gr-1^{hi} population compared to the control antibody treatments (CTRL-light grey line). **(B&C)** Neutrophils (CD11b^{+}Ly6G^{high}) were still depleted at 4 DPI compared to control treated corneas. Corneas were swabbed at 2 and 4 dpi, infectious virus was quantified in a standard virus plaque assay, and data are recorded as pfu/swab ± SEM. Differences between treatment groups were not statistically significant ($p>0.05$) and there was not a significant interaction between the variables of time and treatment (two-way ANOVA with Sidak's post-tests). The data are from a representative experiment that was repeated with similar results

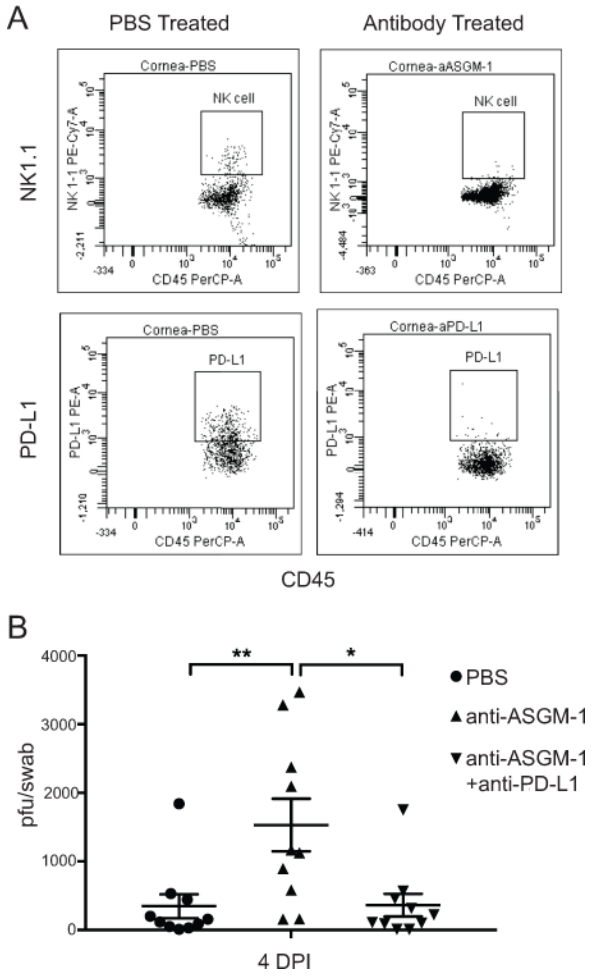

Figure 6. Effect of NK cell depletion on HSV-1 clearance from corneas of B7-H1$^{-/-}$ mice

WT C57BL/6 mice received subconjunctival injections of PBS, anti-ASGM-1 (30ng), or a combination of anti-ASGM-1(30 ng) and anti-PD-L1 (30 ng) 1 day before infection and at 2 dpi. **(A)** Corneas were excised at 6 dpi, single cell suspensions were prepared, stained with antibodies to CD45, NK1.1, and PD-L1 (clone used for in vivo blockade), and analyzed by flow cytometry. Representative flow plots show effective NK cell depletion from corneas (top row) and effective blocking of PD-L1 (bottom row) on CD45^{+} cells. **(B)** Corneas were swabbed 4 days after infection, infectious virus was quantified in a viral plaque assay, and data are recorded as pfu/swab ± SEM. Data were analyzed with a one-way ANOVA with Tukey's post-tests (*$p \leq 0.05$, **$p \leq 0.01$)

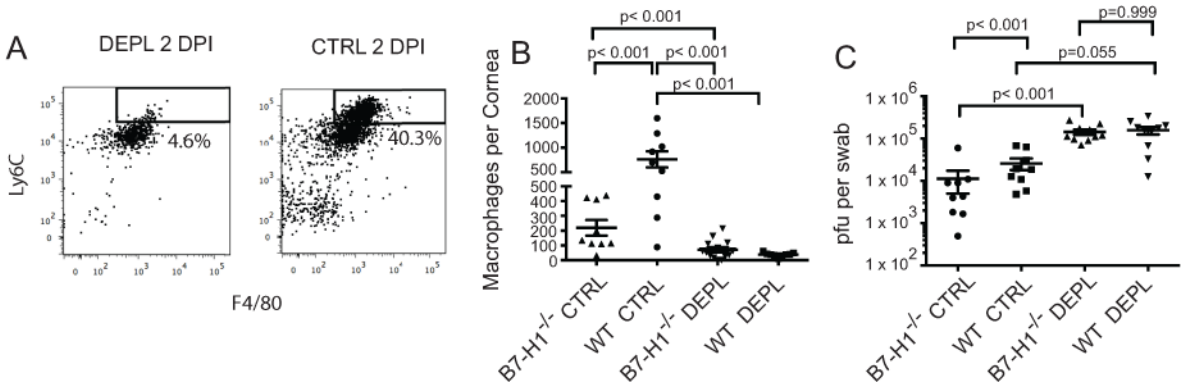

Figure 7. Effect of macrophage depletion on HSV-1 clearance from corneas of B7-H1$^{-/-}$ mice

WT and B7-H1$^{-/-}$ mice received subconjuctival injections with clodronate-liposomes and anti-LY6C antibody (clone MONTS1) or PBS-liposomes immediately before HSV-1 corneal infection. At 2 dpi corneas were excised, single cell suspensions prepared, stained for CD45, Gr-1, F4/80 and CD11b and analyzed by flow cytometry. (**A**) Representative flow plots of corneal cells from WT mice obtained at 2dpi (top panel) gated on CD45 and CD11b show effective depletion of monocytes/macrophages within the Ly6C^{+} and Gr-1$^{int-low}$ gate. (B) Scatter plots based on gates in (A) show significant depletion of macrophages from corneas of WT ($p < 0.05$) and B7-H1$^{-/-}$ ($p < 0.05$) mice at 2dpi (top panel). Data were analyzed by a one-way ANOVA and individual group differences were assessed by a Rank Sum post-hoc test. **(C)** Corneas of macrophage-depleted and mock-depleted (Ctrl) WT and B7-H1$^{-/-}$ mice were swabbed at 2 dpi, infectious virus was quantified in a viral plaque assay, and data recorded as pfu/swab ± SEM. As expected, mock depleted WT mice had higher viral titers than mock depleted B7-H1$^{-/-}$ mice at 2 dpi ($p < 0.001$). Macrophage depletion significantly increased viral titers in both WT and B7-H1$^{-/-}$ mice at 2 dpi, and viral titers were not significantly different in the depleted corneas ($p > 0.05$). Data were log-transformed to normalize the distribution and analyzed with a one-way ANOVA with posttests. The data are from a representative experiment that was repeated twice more with statistically similar results.

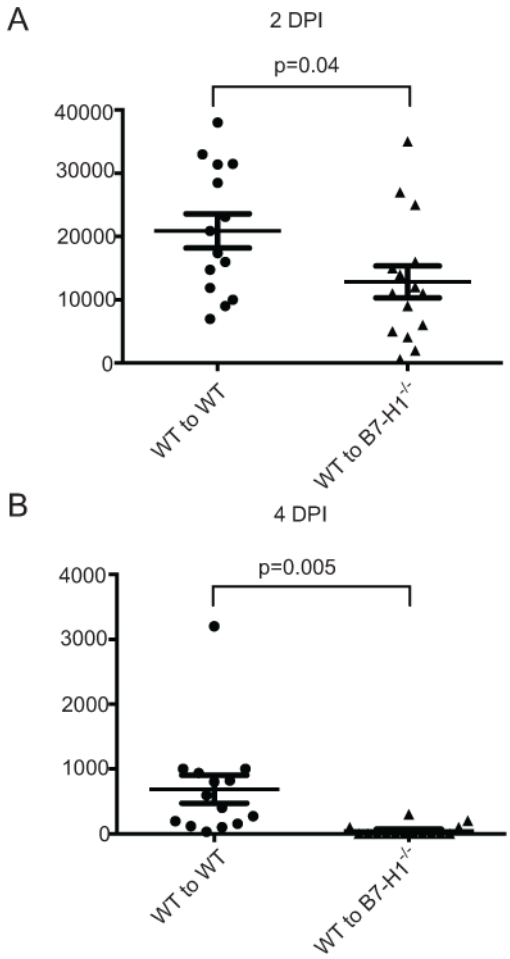

Figure 8. HSV-1 clearance is regulated by PD-L1 expression on non-hematopoetic cells

Chimeric mice were generated by transferring bone marrow from wild type (WT) mice into irradiated WT recipient mice (WT to WT) or to B7-H1$^{-/-}$ recipients (WT to B7-H1$^{-/-}$). The fully reconstituted mice received corneal HSV-1 infections. The infected corneas were swabbed at 2 **(A)** and 4 **(B)** dpi, infectious virus was quantified in a viral plaque assay, and data were recorded as pfu/swab ± SEM. Group differences were statistically significant at both 2 dpi ($p = 0.04$) and 4 dpi ($p = 0.005$) based on unpaired t-tests. Data are pooled from three independent experiments.